OUTER RINGS OF SATURN

J. C. BHATTACHARYYA and R. VASUNDHARA
Indian Institute of Astrophysics, Bangalore 560 034, India

ABSTRACT

A two component model of a possible ring structure at about 12.5 Saturn radii is presented here which can explain the shapes of the immersion and emersion occultation profiles obtained during the occulation of SAO 158913 by Saturn's magnetosphere on March 24, 1984 and March 25, 1984. The four sharp features may be due to micron sized dust grains confined close to the equatorial plane. The extended wings associated with the sharp features may be due to extended ionic and molecular belts stretching far above and below the equatorial plane of the planet Saturn.

THE magnetosphere surrounding the planet Saturn has been known to be quite extensive; the three deep space probes Pioneer XI and Voyagers 1 and 2 have all observed characteristic variations of ion densities and energies in this region[1-6]. Recent observations of occultation of a star by Saturn has yielded clear indications of the presence of absorbing clouds about 12.5 Saturn radii away, close to the equatorial plane. In the present paper results of further critical analysis of the occultation data obtained at Kavalur (Longitude: $-5^h\,15^m\,19.^s6$, Latitude: $+12°\,34'.58$, Height 725 mts.) are presented which throw new light on the physical nature of this circumplanetary matter.

Following the publication of Voyager results, Lazarus *et al*[7] suggested the presence of fine particulate matter in the region of ion density irregularities. Possibilities of detection of such clouds were investigated by Mink[8] who calculated the detailed circumstances of several occultation events when the planet Saturn would drift across some stars. Occultation passages of the star across symmetrical zones in the circumplanetary region during March 24 and 25, 1984 were observed photoelectrically from Kavalur[9,10]. Details of the circumstances and observing equipment have been given in the earlier paper[10].

Two independent scans of the region 12-14 Saturn radii away from the planet centre could be obtained during the events; one on the west side of the planet on March 24 and one on the east side, next day (figure 1). Several interesting features of the extinction light curves suggest a complex structure; these features are discussed below.

Although different wavelength bands were used for the two scans, the general shapes of the light curves were remarkably similar. Large variations in the extinction magnitudes in two spectral bands have been noticed which allow certain interesting speculations regarding the nature of the absorbing clouds. Table 1 summarizes the results of extinction measurements. Observations on the immersion side in white light show a maximum optical depth of 0.71 whereas through blue filter the maximum optical depth as observed next day is only 0.14. Such a variation cannot be explained by a symmetrical model of absorbing clouds.

The extinction of the star beam had occurred at regions symmetrically around the planet's centre. The period during which the extinction was observed was about 40 min on either side of the planet. A close examination of the light curve reveals that the four features which are symmetrical with reference to the Planet's centre, may be ascribed to a concentric system of ringlets in a simplistic model. General feature of these regions are shallow wings culminating in deep central minimum (figures 1, 2). Two of them are quite broad, lasting more than a couple of minutes and have more than one minima embed-

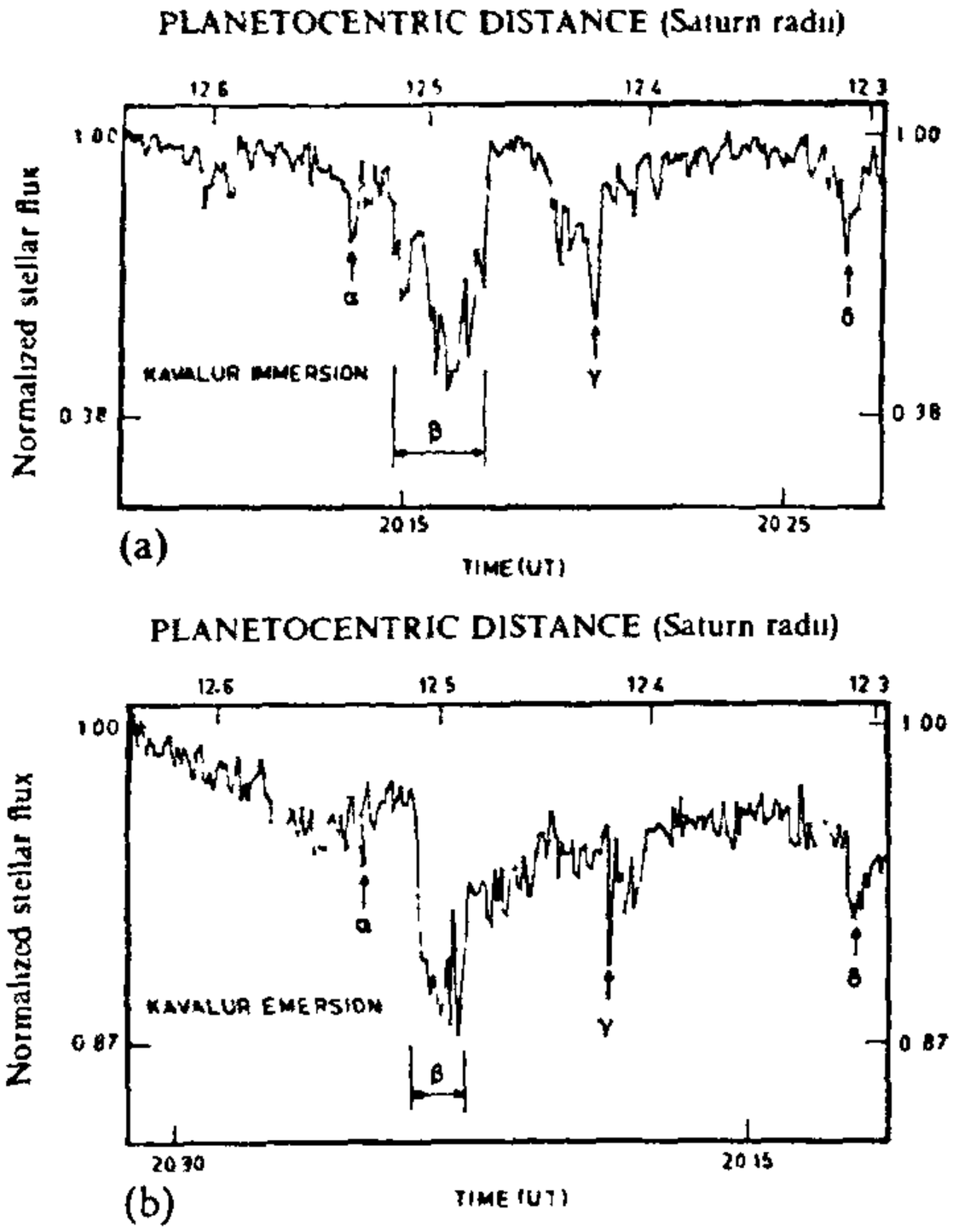

Figure 1. Light curves (a) Immersion on 24 March 1984 (b) Emersion on 25 March 1984, reversed for direct comparison. Each point corresponds to photon counts summed over an interval of 5 seconds.

Table 1 *Optical depth measurements*

Event	Wave-length band	Maximum Optical depth	Overall Optical depth
Immersion 24 March 84 Kavalur	White	.71	.06
Emersion 25 March 84 Kavalur	Blue	.14	.08

Table 2a *Observed timings of the events*

	Immersion – Filter: Clear		Emersion – Filter: Blue	
Event	Observed Timings UT ± a	Duration Sec.	Observed Timings UT ± a	Duration Sec.
Zone	20:11:02.5	420	20:27:20.0	425
Spike	20:13:37.5	≃2	20:24:47.5	≃2
Zone	20:15:57.5	170	20:21:57.5	220
Spike	20:16:44.0	≃2	20:22:49.0	≃1
Zone	20:20.02.5	210	20:17:47.5	110
Spike	20:20:02.5	<1	20:18:25.0	<1
Zone	20:26:25.0	105	20:11:57.5	60
Spike	20:26:36.0	≃2	20:12:09.0	≃3

a = ±5^s for the zones, a = ±1^s for the spikes.

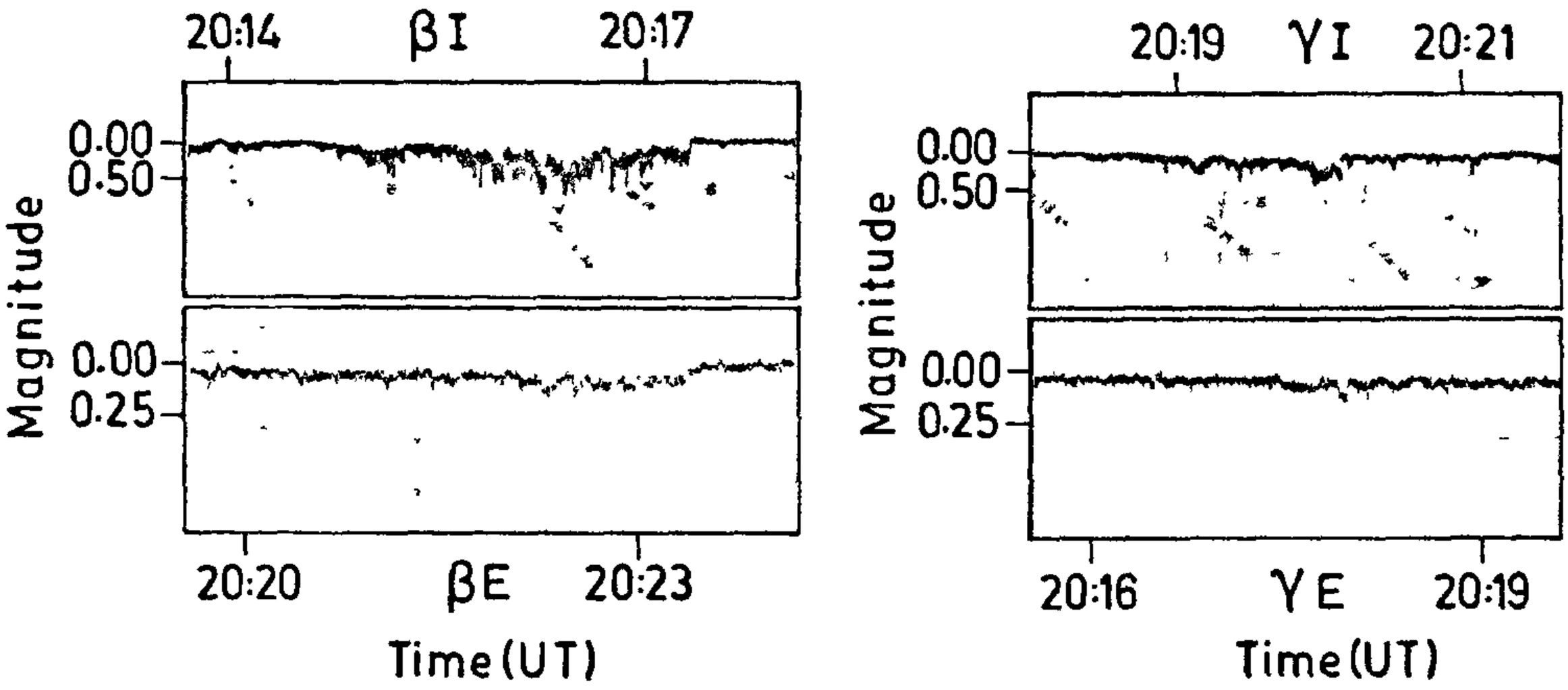

Figure 2. Strip chart recorder tracings showing the dips due to (a) zone β and (b) zone γ. The top figure in each case shows the immersion light curve and the bottom one the emersion light curve. Unlike figure 1 the time axis of emersion light curve is not reversed. Sharp edges on the inner side during immersion and on the outer side during emersion can be clearly noticed on both the curves II(a) and II(b).

Table 2b *Planeto centric distance, width and optical depth of the features*

Event	Immersion			Emersion		
	Planetocentric Distance RS	Width Km	Optical depth	Planetocentric Distance RS	Width Km	Optical depth
Zone	12.5790	7283	.05	12.5756	7565	.07
Spike	12.5344	≃42	.11	12.5307	≃41	.03
Zone	12.4942	2948	.37	12.4805	3916	.12
Spike	12.4808	≃37	.44	12.4957	≃21	.06
Zone	12.4237	3641	.15	12.4067	1958	.10
Spike	12.4237	≃17	.31	12.4178	≃18	.05
Zone	12.3137	1821	.10	12.3036	1068	.11
Spike	12.3106	≃40	.31	12.3069	≃62	.04

ded therein. The other two are relatively thin with the total duration lasting about a minute with one prominent minimum each. The appearance of these features was in a time sequence (table 2a) which unambiguously point to a concentric set of rings. We have designated these by the letters α, β, γ and δ; the details of their calculated widths and optical depths are given in table 2b. The optical depths have been calculated from the magnitudes of the dips below the immediate continuum. The planetocentric distances of the maximum extinction points have been calculated following the method of Elliot *et al*[11]. These are shown alongside in figure 1. It may be noticed that the planetocentric arrangements of these rings are almost perfectly symmetrical. In the absence of timings of occultation events by planet body or any of the known rings to correct for the uncertainty in the relative position of the star and the planet, we find that the planetocentric distances of the four spikes on either side agree even better (in the least square sense) if a correction of $\Delta\alpha = -0^s.0102$ and $\Delta\delta = 0.0$ is applied to the planet position.

Minor variations in the shape within the broad features may, however, be noticed on the two sides of the planet. The minimum light points are not exactly central in the features, and some assymmetry may be seen in the wings. These coupled with the noticed differences in optical depths of the absorbing material indicate that there are large azimuthal variations along the ring plane.

We have also estimated the total extinction over the entire 40 min period and find that the large variations noticed in selected portions of the light curve are considerably reduced in the computation. These integrated optical depths are given in table 1. This suggests the possibility that although the structure is basically symmetrical, other dispersing factors have added to the observed assymmetries.

We have to keep in view that the region in which these absorbing clouds are located are traversed by strong Saturnian magnetic field. Also the deep space probes have detected ionized plasma in the planet's magnetosphere[3]. We also know that the structure of planetary magnetosphere is distorted along the direction of the solar wind. The occulting regions on the two sides of this planet are located in such a way that assymmetries in the distribution of ionised plasma or even fine particles cannot be overruled. The heavier particles are likely to be contained in equatorial planetocentric orbits which may be responsible for the spikes α, β, γ and δ, but the gas and fine dust can extend far out of the equatorial plane giving rise to the broad shallow zones α, β, γ and δ. One feature noticed in our records may be explained if we assume slight assymmetry in the density distribution above and below the equatorial plane of the ring.

This feature is illustrated in figure 2. The wings of the two broad zones β and γ have clearly assymetric profile. On the immersion side inner regions of the rings are sharp while the outer ones

are diffused. The opposite trend is noticed on the emersion side. The shape can be justified if we assume comparatively greater densities of gas and fine dust on the sunlit side of the ring, which appear reasonable from physical causes.

The broad extinction features show deeper extent in broad band white light than in relatively narrower band observations in blue. This is in conflict with the characteristics expected from a pure molecular or particle scattering. We take note of the fact that the gaseous components detected by space probes have deep absorption bands in the visual and red region of the spectrum. The anomalous behaviour of the extinction can be explained by assuming that the same is shared by particulate and gaseous matters, in the ring.

We have made model calculations aiming to explain the qualitative differences in the two extinctions. Assuming equal share of extinction by the two agencies we find that a mixture of micron to submicron sized dirty ice particles immersed in a gaseous medium may explain the differences. A typical concentration of gas molecules by a factor 10^6 over the interplanetary density will be needed to explain the extinction in the wings, which we attribute to gaseous matter.

If we assume that the sharp dips are caused by grains moving in narrow lanes, their space density can be estimated from the extinctions. Assuming a simple model of spherical grains of ice, and using the method developed by Shah[12] we have calculated typical values of column densities for particles of various sizes. These values are given in table 3. It is clear that the observed extinctions can be explained by a column density of 10^7 micron sized particles. If we assume the thickness of this particulate ring in the planet's equatorial plane as 10 km[13], the particle density needed is about 1 particle per cc, a figure which would give a surface density far less than that of B ring of Saturn[14].

We have also estimated the possibility of detection of this ring through ground based observations; in particular we kept in view the negative results of Baron and Elliot[15] in their search of such a particulate ring using a CCD Camera. Reflected Sun light from such a ring has been calculated using the method described by Shah[16] and Wickramasinghe[17] for reflection nebulae. Necessary corrections for extinction and image dilution to take account of the relatively smaller angular size of the sharp features compared to the seeing disc, as applicable in case of Baron and Elliot's observations have been used. Resultant apparent magnitude per square arc second of this ring for the wavelength band of Baron and Elliot's CCD experiment are given in the last column of table 3. It is seen that such a ring should have been marginally detectable; the negative results of their experiment may be attributed, at least partially, to the choice of a telescope system which created strong diffraction bands across the zone of interest.

Combining all these observations we may venture a model of these new possible ring systems. They may consist of two components *viz* a thin set of rings composed of particulate matter in the equatorial plane in the locations of the sharp features surrounded by extended ionic and molecular belts stretching far above and below the equatorial plane in the planet's magnetosphere. The dust rings are responsible for the sharp features and part of the extinction noticed

Table 3 *Column density and expected apparent magnitude of the ring system*

Grain Size microns	Ring material	Refractive Index	Column density per cm^2	Phase function for $\theta = 174°$	Flux received per ergs per cm^2 per sec.	Apparent magnitude per arc sec.square
.4	Dirty ice	$1.33-.05i$	$.25 \times 10^8$	$.1497 \times 10^{-10}$	$.479 \times 10^{-10}$	17.3
.6	"	$1.33-.05i$	$.11 \times 10^8$	$.4671 \times 10^{-10}$	$.0657 \times 10^{-9}$	17
.8	"	$1.33-.05i$	$.08 \times 10^8$	$.1768 \times 10^{-9}$	$.1808 \times 10^{-9}$	16
1.0	"	$1.33-.05i$	$.05 \times 10^8$	$.4535 \times 10^{-10}$	$.2899 \times 10^{-10}$	17.9

in the entire region, whereas the bulk of the extinction is effected by selective absorption by ions and molecules and perhaps by fine dust particles. Such a model can explain the majority of features observed during this particular event.

We wish to thank Drs G. A. Shah and N. Kameswara Rao for useful discussions and Mr. M. Rozario for assistance with the observations at Kavalur Observatory.

21 March 1985

1. Bridge, H. S., Belcher, J. W., Lazarus, A. J., Olbert, S., Sullivan, J. D., Bagenal, F., Gazis, P. R., Hartle, R. E., Ogilvie, K. W., Scudder, J. D., Sittler, E. C., Eviator, A., Siscoe, G. L., Goertz, C. K. and Vasyliunas, V. M., *Science*, 1981, **212**, 217.
2. Krimigis, S. M., Armstrong, T. P., Axford, W. I., Bostrom, C. O., Gloeckler, G., Keath, E. P., Lanzerotti, L. J., Carbary, J. F., Hamilton, D. C. and Roelof, E. C., *Science*, 1981, **212**, 225.
3. Krimigis, S. M., Armstrong, T. P., Axford, W. I., Bostrom, C. O., Gloeckler, G., Keath, E. P., Lanzerotti, L. J., Carbary, J. F., Hamilton, D. C. and Roelof, E. C., *Science*, 1982, **215**, 571.
4. Bridge, H. S., Bagenal, F., Belcher, J. W., Lazarus, A. J., McNutt, R. L., Sullivan, J. D., Gazis, P. R., Hartle, R. E., Ogilvie, K. W., Scudder, J. D., Sittler, E. C., Eviatar, A., Siscoes, G. L., Goertz, C. K. and Vasyliunas, V. M., *Science*, 1982, **215**, 563.
5. Pioneer XI Saturn results, *Science*, 1980, **207**, 400.
6. *J. Geophys. Res.*, 1980, **85**, 561.
7. Lazarus, A. J., Hasegawa, T. and Bagenal, F., *Nature* (*London*), 1983, **302**, 230.
8. Mink, D. J., *Astro. J.*, 1983, **88**, 559.
9. IAU Circ. No. 3941; IAU Circ. No. 3945 (1984).
10. Vasundhara, R., Bhattacharyya, J. C., Santhanam, P., Pande, A. K., Vijay Mohan and Mahra, H. S., *Nature* (*London*), 1984, **312**, 621.
11. Elliot, J. L., Dunham, E., Wasserman, L. H., Millis, R. L. and Churms, J., *Astr. J.*, 1978, **83**, 980.
12. Shah, G. A., *Kodaikanal Obs. Bull. Ser.*, 1977, A**2**, 42.
13. Bobrov, M. S., *A. Zh.*, 1956, **33**, 161, 904.
14. Lane, A. L., Hord, C. W., West, R. A., Esposito, L. W., Coffeen, D. L., Sato, M., Simmons, K. E., Pomphrey, R. B. and Morris, R. B., *Science*, 1982, **215**, 537.
15. Baron, R. L. and Elliot, J. L., *Astr. J.*, 1983, **88**, 562.
16. Shah, G. A., *Pramana*, 1974, **3**, 338.
17. Wickramasinghe, N. C., Interstellar grains, International Astrophysics Series, Chapman and Hall Ltd, 1967, Vol. 9, p. 41.

ANNOUNCEMENT

BATTERY LEAD ALLOYS AND GRID TECHNOLOGY

The Technical Notes Volume contains valuable information, data and diagrams which will be immensely useful to the battery technologists, lead alloy makers, grid and plate manufacturers, shopfloor technicians, foundrymen, lead engineers, metalurgical consultants, research and development personnel.

The compilation serves as a ready reference and may prove a valuable addition to public and personnel technical libraries.

Contents: Grid Alloys – 1. Lead-antimony alloys for battery grids, 2. Low-animonial lead and calcium-lead alloys, 3. Lead alloys for small parts casting, 4. Melting practice and control of lead base alloys and 5. Sampling, quality control and testing of grid metal. Grid fabrication – 6. Cast grids and 7. Wrought grids.

For further details please contact The Battery Society of India, C/o Indian Lead Zinc Information Centre, B-6/7, Shopping Centre, Safdarjung Enclave, New Delhi 110029.